

Spin gap and magnetic resonance in superconducting  $\text{BaFe}_{1.9}\text{Ni}_{0.1}\text{As}_2$ Shiliang Li,<sup>1</sup> Ying Chen,<sup>2</sup> Sung Chang,<sup>2</sup> Jeffrey W. Lynn,<sup>2</sup> Linjun Li,<sup>3</sup> Yongkang Luo,<sup>3</sup> Guanghan Cao,<sup>3</sup> Zhu'an Xu,<sup>3</sup> and Pengcheng Dai<sup>1,4,\*</sup><sup>1</sup>*Department of Physics and Astronomy, The University of Tennessee, Knoxville, Tennessee 37996-1200, USA*<sup>2</sup>*NIST Center for Neutron Research, National Institute of Standards and Technology, Gaithersburg, Maryland 20899, USA*<sup>3</sup>*Department of Physics, Zhejiang University, Hangzhou 310027, China*<sup>4</sup>*Neutron Scattering Science Division, Oak Ridge National Laboratory, Oak Ridge, Tennessee 37831-6393, USA*

(Received 3 February 2009; revised manuscript received 21 April 2009; published 26 May 2009)

We use neutron spectroscopy to determine the nature of the magnetic excitations in superconducting  $\text{BaFe}_{1.9}\text{Ni}_{0.1}\text{As}_2$  ( $T_c=20$  K). Above  $T_c$  the excitations are gapless and centered at the commensurate antiferromagnetic wave vector of the parent compound, while the intensity exhibits a sinusoidal modulation along the  $c$  axis. As the superconducting state is entered a spin gap gradually opens, whose magnitude tracks the  $T$  dependence of the superconducting gap as observed by angle-resolved photoemission. Both the spin-gap and magnetic-resonance energies are temperature *and* wave-vector dependent, but their ratio is the same within uncertainties. These results suggest that the spin resonance is a singlet-triplet excitation related to electron pairing and superconductivity.

DOI: [10.1103/PhysRevB.79.174527](https://doi.org/10.1103/PhysRevB.79.174527)

PACS number(s): 74.25.Ha, 74.25.Jb, 78.70.Nx

## I. INTRODUCTION

The magnetic scattering in the high-transition-temperature (high- $T_c$ ) copper oxide superconductors is characterized by strong spin correlations in the vicinity of the antiferromagnetic (AF) wave vector of the magnetically ordered parent materials and a spin-“resonant” magnetic excitation whose energy scales with  $T_c$  and whose intensity develops like the superconducting order parameter.<sup>1-4</sup> Like the cuprates, the Fe-based superconductors<sup>5-7</sup> are derived from electron<sup>8-11</sup> or hole<sup>12</sup> doping of their AF long-ranged ordered parent compounds<sup>13-18</sup> and spin fluctuations have been postulated as the possible glue for mediating the electron pairing for superconductivity.<sup>19-21</sup> Indeed, the very recent observation of the same type of magnetic-resonant excitation in the iron-based superconductors<sup>22-24</sup> inexorably links these two high- $T_c$  superconductor families together and strongly suggests that the pairing mechanism has a common origin that is intimately tied to the magnetic properties.

An essential step in elucidating the role of magnetism in the superconductivity of these materials is then an in-depth determination of the energy ( $E=\hbar\omega$ ) and wave-vector ( $Q$ ) dependence of the low-energy magnetic scattering as the superconducting state is formed.<sup>19-21</sup> If electrons in the Fe-based superconductors indeed form pairs of spin singlets below  $T_c$  as in conventional superconductors<sup>25</sup> and high- $T_c$  copper oxides, there can be an energy associated with exciting the spin singlet into the high-energy spin-triplet state without unbinding the electron pairs. In this picture, the Cooper pairs should exhibit a wave-vector-independent spin gap with a  $T$  dependence that gradually opens below  $T_c$ , much like the temperature dependence of the isotropic superconducting gap function observed by angle-resolved photoemission spectroscopy (ARPES) experiments.<sup>26,27</sup> We have used inelastic neutron scattering to probe the wave-vector and energy dependence of the low-energy magnetic-excitation spectrum  $S(Q, \omega)$ . We find that the spin gap does open gradually below  $T_c$  but the gap energy is dispersive rather than

wave-vector independent and tracks the dispersion of the resonant mode that has been observed.<sup>24</sup> These results suggest that the resonant mode is indeed the spin singlet to spin-triplet excitation.

We chose single crystals of superconducting  $\text{BaFe}_{1.9}\text{Ni}_{0.1}\text{As}_2$  (with onset  $T_c=20$  K and transition width  $\Delta T_c < 2$  K) because these samples have excellent superconducting properties.<sup>11</sup> In the absence of Ni doping,  $\text{BaFe}_2\text{As}_2$  is a nonsuperconducting metal that orders antiferromagnetically with a spin structure shown in Fig. 1(a).<sup>16</sup> Because of the unit-cell doubling along the orthorhombic  $a$ -axis and  $c$ -axis spin arrangements, magnetic Bragg reflections occur at wave vectors  $Q=(1, 0, 1)$ - and  $(1, 0, 3)$ -type positions and are absent at  $Q=(1, 0, 0)$  and  $(1, 0, 2)$ .<sup>16-18</sup> Previous neutron-scattering experiments on hole-doped  $\text{Ba}_{0.86}\text{K}_{0.4}\text{Fe}_2\text{As}_2$  powder samples<sup>22</sup> and single crystals of  $\text{BaFe}_{1.84}\text{Co}_{0.16}\text{As}_2$  ( $T_c=22$  K) (Ref. 23) have shown that the effect of superconductivity is to induce a neutron spin resonance at energies of  $\sim 5k_B T$ , remarkably similar to the doping dependence of the resonance in high- $T_c$  copper oxides<sup>28,29</sup> and heavy fermions.<sup>30,31</sup> Measurements on single crystals of  $\text{BaFe}_{1.9}\text{Ni}_{0.1}\text{As}_2$  ( $T_c=20$  K) (Ref. 24) suggest that the resonance actually exhibits dispersion along the  $c$  axis and occurs at distinctively different energies at the three-dimensional (3D) AF ordering wave vector  $Q=(1, 0, 1)$  and at  $Q=(1, 0, 0)$ . We note that in the parent materials the spin-wave dispersions in the Fe-based superconductors are anisotropic and clearly 3D in nature, as opposed to the purely two-dimensional (2D) spin-wave dispersion on the parent cuprates. For the cuprates the spin fluctuations in the superconducting regime are again purely 2D,<sup>28,29,32</sup> while the iron-based superconductors appear to exhibit anisotropic 3D behavior like their parents.

## II. EXPERIMENTS

The neutron-scattering measurements were carried out on the SPINS cold and BT-7 thermal triple-axis spectrometers at

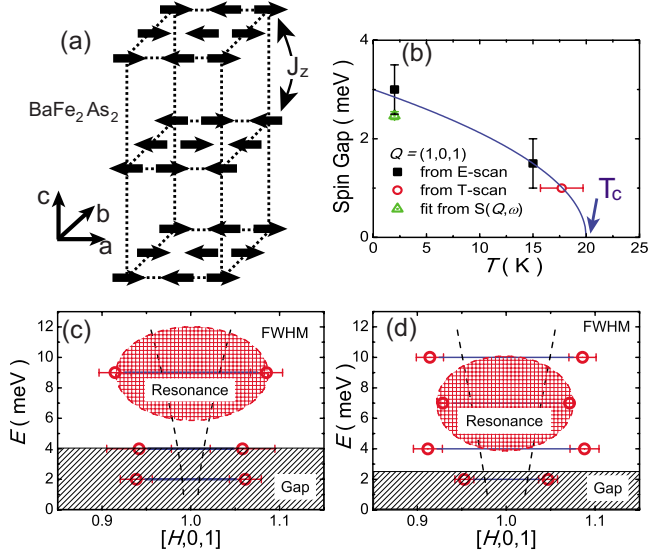


FIG. 1. (Color online) (a) Schematic of the Fe spin structure in the BaFe<sub>2</sub>As<sub>2</sub> which has magnetic Bragg peaks at  $Q=(1,0,1)$ ,  $(1,0,3)$ , etc. For our experiment on BaFe<sub>1.9</sub>Ni<sub>0.1</sub>As<sub>2</sub>, we use the same unit cell for easy comparison. (b) Temperature dependence of the spin gap as determined from energy scans [Fig. 3(c)] and the temperature dependence of the scattering at  $Q=(1,0,1)$  [Fig. 3(d)]. The solid curve represents the temperature dependence of the BCS gap function. [(c) and (d)] Schematic of the magnetic response and spin gaps at  $Q=(1,0,0)$ , and  $(1,0,1)$ , respectively. Measurements at  $Q=(1,0,3)$  showed similar behavior as those at  $Q=(1,0,1)$ .

the NIST Center for Neutron Research. The sample was measured in the liquid-helium cryostat with a temperature control better than 0.01 K below 30 K. We label the momentum transfer  $Q=(q_x, q_y, q_z)$  as  $(H, K, L) = (q_x a/2\pi, q_y b/2\pi, q_z c/2\pi)$  reciprocal lattice units (rlu) using the orthorhombic magnetic unit cell of the parent undoped compound (space group  $Fmmm$ ,  $a=5.564$ ,  $b=5.564$ , and  $c=12.77$  Å) for easy comparison with previous spin-wave measurements on the parent compounds even though the actual crystal structure is tetragonal.<sup>33–35</sup> Many single crystals were coaligned to obtain a total mass of  $\sim 1.2$  grams. The in-plane and out-of-plane mosaics of the aligned crystal assembly are  $1.3^\circ$  and  $4.3^\circ$  full width at half maximum, respectively.<sup>24</sup> For the experiment, the BaFe<sub>1.9</sub>Ni<sub>0.1</sub>As<sub>2</sub> crystal assembly was mounted in the  $[H,0,L]$  zone inside a liquid He cryostat. The final neutron wave vector was fixed at either  $E_f=5$  meV with a cold Be filter or at  $E_f=14.7$  meV with a pyrolytic graphite filter in front of the analyzer.

### III. RESULTS AND DISCUSSIONS

We first probe the wave-vector dependence of the low-energy spin fluctuations. Figures 2(a) and 2(b) show  $[H,0,3]$  and  $[1,0,L]$  scans at  $E=1$  meV through the 3D  $(1,0,3)$  Bragg-peak position below and above  $T_c$ . From other measurements taken at different  $Q$  [e.g.,  $(1,0,1)$ ] or energies (e.g., 2 meV) at either the same spectrometer or other spectrometers,<sup>24</sup> we see that the spin excitations above  $T_c$  are

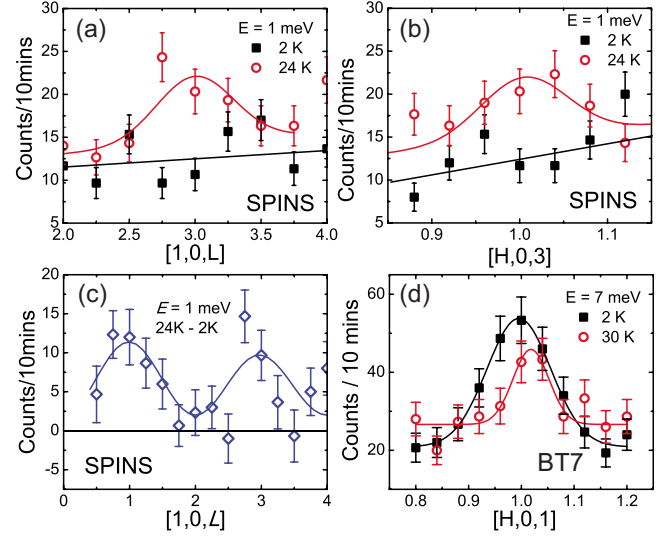


FIG. 2. (Color online) Examples of constant energy scans around the  $(1,0,3)$  position for  $E=1$  meV obtained with  $E_f=5$  meV above and below  $T_c$  on SPINS. (a)  $Q$  scan along the  $[1,0,L]$  direction for  $E=1$  meV at 24 and 2 K. A clear peak centered at  $(1,0,3)$  at 24 K disappears at 2 K, indicating the opening of a spin gap. (b) Similar scan along the  $[H,0,3]$  direction showing a peak centered at  $(1,0,3)$  that disappears below  $T_c$ . (c) Using scattering at 2 K as background scattering, we determine the normal-state  $L$  modulation of the spin fluctuations by subtracting the 2 K data from 24 K data. It is clear that spin fluctuations are 3D and have similar modulations along the  $c$  axis as spin waves. (d)  $Q$  scan in the superconducting state through the magnetic-resonance position and above  $T_c$  near  $(1,0,1)$ .

unobservable at low  $T$ , suggesting a full gap. Figure 2(c) shows the intensity of the scattering above  $T_c$  as a function of wave vector along the  $c$  axis, using the low  $T$  data as background, and reveals the intrinsic wave-vector modulation of the intensity of the normal-state spin fluctuations. The solid curve is a fit to the data using  $\Delta S(Q, \omega)(24 \text{ K} - 2 \text{ K}) = AF(Q)^2 \sin^2(\pi L/2) + C$ , where  $F(Q)$  is the magnetic-form factor of Fe<sup>2+</sup> and  $C$  is constant. These data are consistent with previous work on BaFe<sub>1.9</sub>Ni<sub>0.1</sub>As<sub>2</sub> which showed that the spin-fluctuation intensity has a  $c$ -axis modulation at  $E=8.5$  meV and a gap in the superconducting state.<sup>24</sup> For comparison, Fig. 2(d) shows the magnetic scattering through the  $[1,0,1]$  position in the superconducting state at the resonance energy of  $E=7$  meV and the magnetic scattering above  $T_c$ . We note that in the undoped AF state, the spin-wave spectrum in BaFe<sub>2</sub>As<sub>2</sub> has a gap of 9.8 meV (Ref. 35) while in the normal state of the doped system we find that the spin-fluctuation spectrum is gapless.

The behavior of the low-energy spin excitations as a function of temperature is shown in Fig. 3, which summarizes the BT-7 and SPINS data around  $Q=(1,0,1)$ . Figure 3(a) shows wave vector  $[H,0,1]$  scans through the  $Q=(1,0,1)$  position above and below  $T_c$  at  $E=2$  meV. A clear Gaussian peak centered at  $Q=(1,0,1)$  in the normal state vanishes below  $T_c$ , suggesting that the spin gap  $\Delta_{\text{spin}} > 2$  meV. Figure 3(b) plots the signal and background scattering along the  $[1,0,L]$  direction for  $E=2$  meV at 30 K, where we find that the normal-state scattering also peaks at 3D AF wave-vector po-

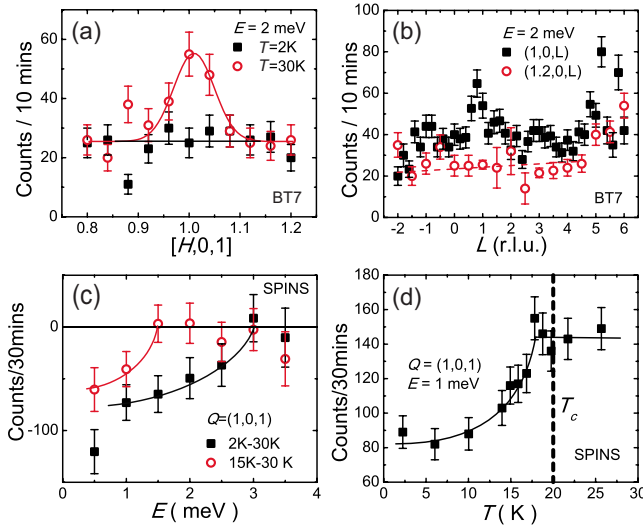


FIG. 3. (Color online) (a)  $Q$  scans at the  $[H,0,1]$  direction above and below  $T_c$  at  $\hbar\omega=2$  meV. The data show the opening of a spin gap at 2 meV below  $T_c$ . (b)  $Q$  scans along the  $[1,0,L]$  (signal) and  $[1.2,0,L]$  (background) positions, showing the  $L$  modulation of the intensity with maxima at  $(1,0,1)$  and  $(1,0,3)$ . (c) Constant  $Q$  scans at  $Q=(1,0,1)$  at various temperatures. The differences between low- and high-temperature data show negative scattering due to the opening of a spin gap. The data suggest a spin-gap value of 1.5 meV at 15 K and 3.0 meV at 2 K. (d) Temperature dependence of the scattering at  $Q=(1,0,1)$  and  $E=1$  meV shows a sudden drop below 18 K ( $=T_c-2$  K) suggesting that the  $E=1$  meV spin gap opens at a temperature slightly below  $T_c$ .

sitions. To determine the spin-gap value at  $Q=(1,0,1)$ , we carried out temperature-dependent constant- $Q$  measurements at 2, 15, and 30 K using SPINS. We find a clear reduction in scattering (net negative values in the subtraction) below 3 and 1.5 meV at 2 and 15 K, respectively. These results show that the maximal observed magnitude of the spin gap at the  $Q=(1,0,1)$  wave vector is  $3 \pm 0.5$  meV, where the error bar is estimated as measuring energy step and the energy gap is temperature dependent.

To quantitatively determine the wave-vector dependence of the spin gap in the superconducting state, we carried out constant- $Q$  scans at the  $Q=(1,0,0)$  and  $(1,0,1)$  wave vectors, and collected background data at  $Q=(1.2,0,0)$ ,  $(1.2,0,1)$ , and above and below  $T_c$  [Figs. 4(a) and 4(b)]. In the normal state (open circles) the magnetic scattering above background at both  $Q=(1,0,0)$  and  $(1,0,1)$  appears to increase with decreasing energy near the elastic line and thus suggests that this component of the scattering is quasielastic in nature (peaks at  $E=0$ ). In the superconducting state (solid squares), the low-energy scattering is suppressed, while the higher-energy scattering increases in intensity. The overall behavior of the data is remarkably similar to that in the optimally hole-doped  $\text{La}_{1-x}\text{Sr}_x\text{CuO}_4$  (Ref. 32) and electron-doped  $\text{Nd}_{1.85}\text{Ce}_{0.15}\text{CuO}_4$ .<sup>29</sup> However, it is also clear that the spin gap occurs at a lower energy at  $Q=(1,0,1)$  than for  $Q=(1,0,0)$ , which is quite different than the cuprates.<sup>32</sup> Figures 4(c) and 4(d) present the data in the form of the dynamic susceptibility  $\chi''(Q, \omega)$ , which is related to  $S(Q, \omega)$

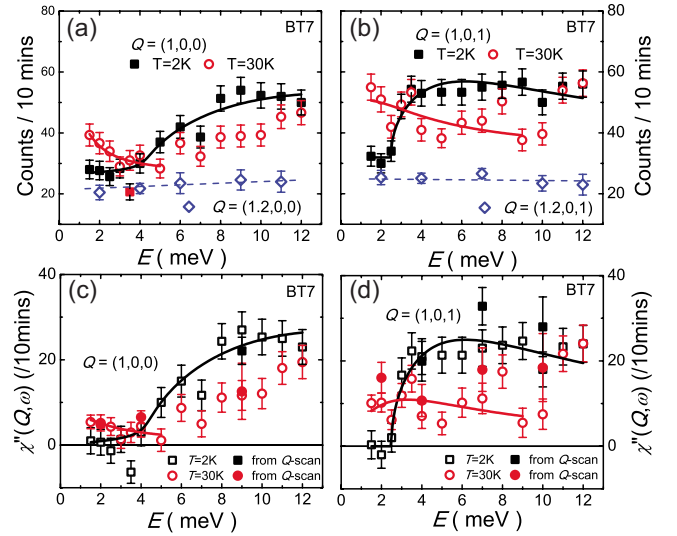


FIG. 4. (Color online) Constant  $Q$  scans around the (a)  $Q=(1,0,0)$  and (b)  $(1,0,1)$  positions above and below  $T_c$ , showing the development of the spin gap at low energies, and the enhancement of the magnetic scattering at the resonance energy at each wave vector. Background data are indicated by the open diamonds and dashed curves, and were collected at  $Q=(1.2,0,0)$  and  $Q=(1.2,0,1)$ , respectively. [(c) and (d)]  $\chi''(Q, \omega)$  above and below  $T_c$  obtained by subtracting background and removing the thermal factor (see text). Also shown are values obtained from the constant  $E$  scans at various energies above and below  $T_c$ , which are consistent with the results of constant  $Q$  scans, suggesting that the subtracted results are reliable. At both wave vectors there is a clear magnetic intensity gain at the resonance energy of  $E=9.0$  meV at  $Q=(1,0,0)$  and 7 meV at  $Q=(1,0,1)$  and spin gaps of 4.3 and 2.5 meV, respectively. The solid lines show fits using the model described in the text.

through the (removal of the) detailed balance factor;  $\chi''(Q, \omega) = [1 - \exp(-\hbar\omega/k_B T)] S(Q, \omega)$ . Recall that the thermal population factor increases with decreasing temperature, and this function is divided into  $S(Q, \omega)$  to obtain  $\chi''(Q, \omega)$  [with  $\chi''(Q, \omega=0)=0$ ]. The filled circles are  $\chi''(Q, \omega)$  obtained from  $Q$  scans as a consistency check. Upon entering the superconducting state, the spectral weight is rearranged with the suppression of low-energy spin fluctuations and the appearance of the neutron spin resonance at energies above the spin gap. The present data give the spin-resonance values at  $Q=(1,0,0)$  and  $Q=(1,0,1)$  are  $8.7 \pm 0.4$  and  $7.2 \pm 0.7$  meV, respectively, which are consistent with the previously reported values.<sup>24</sup> We estimate that the intensity of the resonance is approximately compensated by the opening of the spin gap below the resonance.

To quantify the magnitude of the spin gaps at  $Q=(1,0,0)$  and  $(1,0,1)$  in the superconducting state, we follow previous work<sup>32</sup> and fit the data with

$$S(Q, \omega) = \frac{AE'\Gamma}{[\Gamma^2 + (\hbar\omega)^2][1 - \exp(-\hbar\omega/k_B T)]}, \quad (1)$$

where  $E' = \text{Re}[(\hbar\omega - \Delta + i\Gamma_s)(\hbar\omega + \Delta + i\Gamma_s)]^{1/2}$ ,  $A$  is the amplitude,  $\Delta$  is the spin gap,  $\Gamma$  is the inverse lifetime of the spin fluctuations with  $\hbar\omega \gg \Delta$ ,  $E'$  is an odd function of  $E = \hbar\omega$ ,

and  $\Gamma_s$  is the inverse lifetime of the fluctuations at the gap edge. The solid curves are the results of these fits. In the normal state, this functional form does not provide an adequate fit over the entire energy range, and we restricted it to lower energies (as indicated by the extent of the curve for those data). We find  $\Delta=0$  for both  $Q=(1,0,0)$  and  $(1,0,1)$ . On cooling into the superconducting state, Eq. (1) can be used over the entire energy range of the data, and the least squares fit to the  $Q=(1,0,0)$  data [solid curves in Figs. 4(a) and 4(c)] yields  $A=56.7 \pm 7.9$ ,  $\Gamma=13 \pm 6.5$  meV,  $\Delta=4.3 \pm 0.8$  meV, and  $\Gamma_s=0 \pm 0.73$  meV. Similarly, for  $Q=(1,0,1)$  we find  $A=55.5 \pm 14.5$ ,  $\Gamma=5 \pm 0.7$  meV,  $\Delta=2.5 \pm 0.08$  meV, and  $\Gamma_s=0 \pm 0.53$  meV [solid curves in Figs. 4(b) and 4(d)]. The results of this analysis show that the superconducting spin-gap values for  $Q=(1,0,0)$  and  $(1,0,1)$  are distinctively different. These values are smaller than the value determined from empirical relation  $E_{sg}=3.8k_B T_c$  in YBCO.<sup>3</sup> It should be pointed out that more detailed study is needed to obtain more reliable quantitative results, especially those in the normal state.

The present measurements, as well as the previous data on this material,<sup>24</sup> demonstrate that both the resonance energy and spin-gap value at  $Q=(1,0,0)$  are larger than those at  $Q=(1,0,1)$ . Using the values given above, we obtain the ratio between these two energy scales at  $Q=(1,0,0)$  and  $Q=(1,0,1)$  are  $2.0 \pm 0.4$  and  $2.9 \pm 0.3$ , respectively. Broadly speaking, these two energy scales track one another with ratios that are close to each other within the uncertainties of the experiments. This is the expected behavior for the singlet-triplet transition of a Cooper pair.<sup>36</sup> However, it is

necessary to have better statistics to really pin down this loose speculation.

We summarize in Figs. 1(b)–1(d) the key results of our experiments. The measured temperature dependence of the spin gap at  $Q=(1,0,1)$  is shown in Fig. 1(b). The solid curve shows the prediction of a simple BCS gap function near  $T_c$ ,  $\Delta(T)=A[1-(T/T_c)]^{1/2}$ , which describes the data fairly well. Figures 1(c) and 1(d) plot schematically the spin gap and resonance at  $Q=(1,0,0)$  and  $(1,0,1)$ . The two energies exhibit the same dependence on wave vector. In ARPES experiments,<sup>27</sup> two isotropic superconducting gaps with values of 7 and 4.5 meV were observed for  $\text{BaFe}_{1.85}\text{Co}_{0.15}\text{As}_2$  with  $T_c=25.5$  K. Comparison with the  $Q=(1,0,0)$  neutron measurements suggests that the resonance energy at  $Q=(1,0,0)$  is indeed less than twice the superconducting gap energy. These results are consistent with the idea that the resonance is a bond state related to singlet-triplet excitations of Cooper pairs with a superconducting gap that varies with the momentum transfer along the  $c$  axis.<sup>36</sup>

#### ACKNOWLEDGMENTS

We thank Songxue Chi, Jun Zhao, and Leland Harriger for coaligning some of the single crystals used in the present experiment. This work is supported by the U.S. DOE BES under Grant No. DE-FG02-05ER46202, NSF under Grant No. DMR-0756568, and in part by the U.S. DOE, Division of Scientific User Facilities. The work at Zhejiang University is supported by the NSF of China. This work utilized facilities supported in part by the National Science Foundation under Agreement No. DMR-0454672.

\*daip@ornl.gov

<sup>1</sup>J. Rossat-Mignod, L. P. Regnault, C. Vettier, P. Bourges, P. Burlet, J. Bossy, J. Y. Henry, and G. Lapertot, *Physica C* **185-189**, 86 (1991).

<sup>2</sup>H. A. Mook, M. Yethiraj, G. Aeppli, T. E. Mason, and T. Armstrong, *Phys. Rev. Lett.* **70**, 3490 (1993).

<sup>3</sup>P. Dai, H. A. Mook, R. D. Hunt, and F. Dogan, *Phys. Rev. B* **63**, 054525 (2001).

<sup>4</sup>C. Stock, W. J. L. Buyers, R. Liang, D. Peets, Z. Tun, D. Bonn, W. N. Hardy, and R. J. Birgeneau, *Phys. Rev. B* **69**, 014502 (2004).

<sup>5</sup>C. K. Xu and S. Sachdev, *Nat. Phys.* **4**, 898 (2008).

<sup>6</sup>M. R. Norman, *Physics* **1**, 21 (2008).

<sup>7</sup>S. A. Kivelson and H. Yao, *Nature Mater.* **7**, 927 (2008).

<sup>8</sup>Y. Kamihara, T. Watanabe, M. Hirano, and H. Hosono, *J. Am. Chem. Soc.* **130**, 3296 (2008).

<sup>9</sup>A. Leithe-Jasper, W. Schnelle, C. Geibel, and H. Rosner, *Phys. Rev. Lett.* **101**, 207004 (2008).

<sup>10</sup>A. S. Sefat, R. Jin, M. A. McGuire, B. C. Sales, D. J. Singh, and D. Mandrus, *Phys. Rev. Lett.* **101**, 117004 (2008).

<sup>11</sup>L. J. Li, Q. B. Wang, Y. K. Luo, H. Chen, Q. Tao, Y. K. Li, X. Lin, M. He, Z. W. Zhu, G. H. Cao, and Z. A. Xu, *New J. Phys.* **11**, 025008 (2009).

<sup>12</sup>M. Rotter, M. Tegel, and D. Johrendt, *Phys. Rev. Lett.* **101**,

107006 (2008).

<sup>13</sup>C. de la Cruz, Q. Huang, J. W. Lynn, J. Li, W. Ratcliff, J. L. Zarestky, H. A. Mook, G. F. Chen, J. L. Luo, N. L. Wang, and P. Dai, *Nature (London)* **453**, 899 (2008).

<sup>14</sup>M. A. McGuire, A. D. Christianson, A. S. Sefat, B. C. Sales, M. D. Lumsden, R. Jin, E. A. Payzant, D. Mandrus, Y. Luan, V. Keppens, V. Varadarajan, J. W. Brill, R. P. Hermann, M. T. Sougrati, F. Grandjean, and G. J. Long, *Phys. Rev. B* **78**, 094517 (2008).

<sup>15</sup>J. Zhao, Q. Huang, C. de la Cruz, S. Li, J. W. Lynn, Y. Chen, M. A. Green, G. F. Chen, G. Li, Z. Li, J. L. Luo, N. L. Wang, and P. Dai, *Nature Mater.* **7**, 953 (2008).

<sup>16</sup>Q. Huang, Y. Qiu, W. Bao, M. A. Green, J. W. Lynn, Y. C. Gasparovic, T. Wu, G. Wu, and X. H. Chen, *Phys. Rev. Lett.* **101**, 257003 (2008).

<sup>17</sup>J. Zhao, W. Ratcliff, J. W. Lynn, G. F. Chen, J. L. Luo, N. L. Wang, J. Hu, and P. Dai, *Phys. Rev. B* **78**, 140504(R) (2008).

<sup>18</sup>A. I. Goldman, D. N. Argyriou, B. Ouladdiaf, T. Chatterji, A. Kreyssig, S. Nandi, N. Ni, S. L. Bud'ko, P. C. Canfield, and R. J. McQueeney, *Phys. Rev. B* **78**, 100506(R) (2008).

<sup>19</sup>I. I. Mazin and J. Schmalian, *Physica C* **469**, 614 (2009).

<sup>20</sup>A. V. Chubukov, D. V. Efremov, and I. Eremin, *Phys. Rev. B* **78**, 134512 (2008).

<sup>21</sup>V. Stanev, J. Kang, and Z. Tesanovic, *Phys. Rev. B* **78**, 184509

- (2008).
- <sup>22</sup>A. D. Christianson, E. A. Goremychkin, R. Osborn, S. Rosenkranz, M. D. Lumsden, C. D. Malliakas, I. S. Todorov, H. Claus, D. Y. Chung, M. G. Kanatzidis, R. I. Bewley, and T. Guidi, *Nature (London)* **456**, 930 (2008).
- <sup>23</sup>M. D. Lumsden, A. D. Christianson, D. Parshall, M. B. Stone, S. E. Nagler, G. J. MacDougall, H. A. Mook, K. Lokshin, T. Egami, D. L. Abernathy, E. A. Goremychkin, R. Osborn, M. A. McGuire, A. S. Sefat, R. Jin, B. C. Sales, and D. Mandrus, *Phys. Rev. Lett.* **102**, 107005 (2009).
- <sup>24</sup>S. Chi, A. Schneidewind, J. Zhao, L. W. Harriger, L. Li, Y. Luo, G. Cao, Z. Xu, M. Loewenhaupt, J. Hu, and P. Dai, *Phys. Rev. Lett.* **102**, 107006 (2009).
- <sup>25</sup>J. Bardeen, L. N. Cooper, and J. R. Schrieffer, *Phys. Rev.* **108**, 1175 (1957).
- <sup>26</sup>H. Ding, P. Richard, K. Nakayama, K. Sugawara, T. Arakane, Y. Sekiba, A. Takayama, S. Souma, T. Sato, T. Takahashi, Z. Wang, X. Dai, Z. Fang, G. F. Chen, J. L. Luo, and N. L. Wang, *Europhys. Lett.* **83**, 47001 (2008).
- <sup>27</sup>K. Terashima, Y. Sekiba, J. H. Bowen, K. Nakayama, T. Kawahara, T. Sato, P. Richard, Y.-M. Xu, L. J. Li, G. H. Cao, Z.-A. Xu, H. Ding, and T. Takahashi, *Proc. Natl. Acad. Sci. U.S.A.*, **106**, 7330 (2009).
- <sup>28</sup>S. D. Wilson, P. Dai, S. Li, S. Chi, H. J. Kang, and J. W. Lynn, *Nature (London)* **442**, 59 (2006).
- <sup>29</sup>J. Zhao, P. Dai, S. Li, P. G. Freeman, Y. Onose, and Y. Tokura, *Phys. Rev. Lett.* **99**, 017001 (2007).
- <sup>30</sup>N. Metoki, Y. Haga, Y. Koike, and Y. Onuki, *Phys. Rev. Lett.* **80**, 5417 (1998).
- <sup>31</sup>C. Stock, C. Broholm, J. Hudis, H. J. Kang, and C. Petrovic, *Phys. Rev. Lett.* **100**, 087001 (2008).
- <sup>32</sup>B. Lake, G. Aeppli, T. E. Mason, A. Schröder, D. F. McMorrow, K. Lefmann, M. Isshiki, M. Nohara, H. Takagi, and S. M. Hayden, *Nature (London)* **400**, 43 (1999).
- <sup>33</sup>J. Zhao, D. X. Yao, S. Li, T. Hong, Y. Chen, S. Chang, W. Ratcliff, J. W. Lynn, H. A. Mook, G. F. Chen, J. L. Luo, N. L. Wang, E. W. Carlson, J. Hu, and P. Dai, *Phys. Rev. Lett.* **101**, 167203 (2008).
- <sup>34</sup>R. J. McQueeney, S. O. Diallo, V. P. Antropov, G. D. Samolyuk, C. Broholm, N. Ni, S. Nandi, M. Yethiraj, J. L. Zarestky, J. J. Pulikkotil, A. Kreyssig, M. D. Lumsden, B. N. Harmon, P. C. Canfield, and A. I. Goldman, *Phys. Rev. Lett.* **101**, 227205 (2008).
- <sup>35</sup>K. Matan, R. Morinaga, K. Iida, and T. J. Sato, *Phys. Rev. B* **79**, 054526 (2009).
- <sup>36</sup>M. Eschrig, *Adv. Phys.* **55**, 47 (2006).